THE UNIVERSITY OF TEXAS AT AUSTIN

Presentation at Baker Hughes
January 15, 2008

Towards Accurate Simulations of AC Dual-Laterolog Measurements with Tool Eccentricity Using *hp*-Finite Elements

M. J. Nam, D. Pardo, C. Torres-Verdín, M. Paszynski

Center for Petroleum and Geosystems Engineering

The University of Texas at Austin

Outline

- Previous Work: 2D Dual-Laterolog (DLL)
  - *hp* Adaptive Finite Element Method
  - Embedded Post-Processing Method
- 3D Methodology and DLL Simulations
  - Deviated Wells
  - Eccentered Measurements
  - Iterative Solver
  - Parallel Implementation
- Conclusions and Future Work

hp-FEM

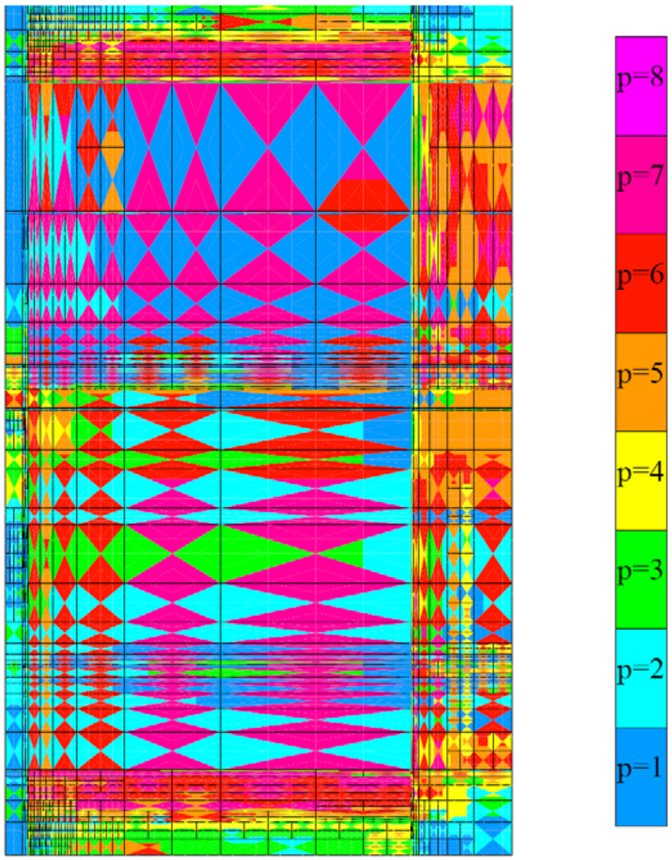

We vary locally the element size *h* and the polynomial order of approximation *p* throughout the grid

Optimal grids are automatically generated by the hp-algorithm

The self-adaptive goal-oriented *hp*-FEM provides exponential convergence rates in terms of the CPU time vs. the error in a user prescribed quantity of interest

Dual-Laterolog (DLL)

- **Description of Tool**

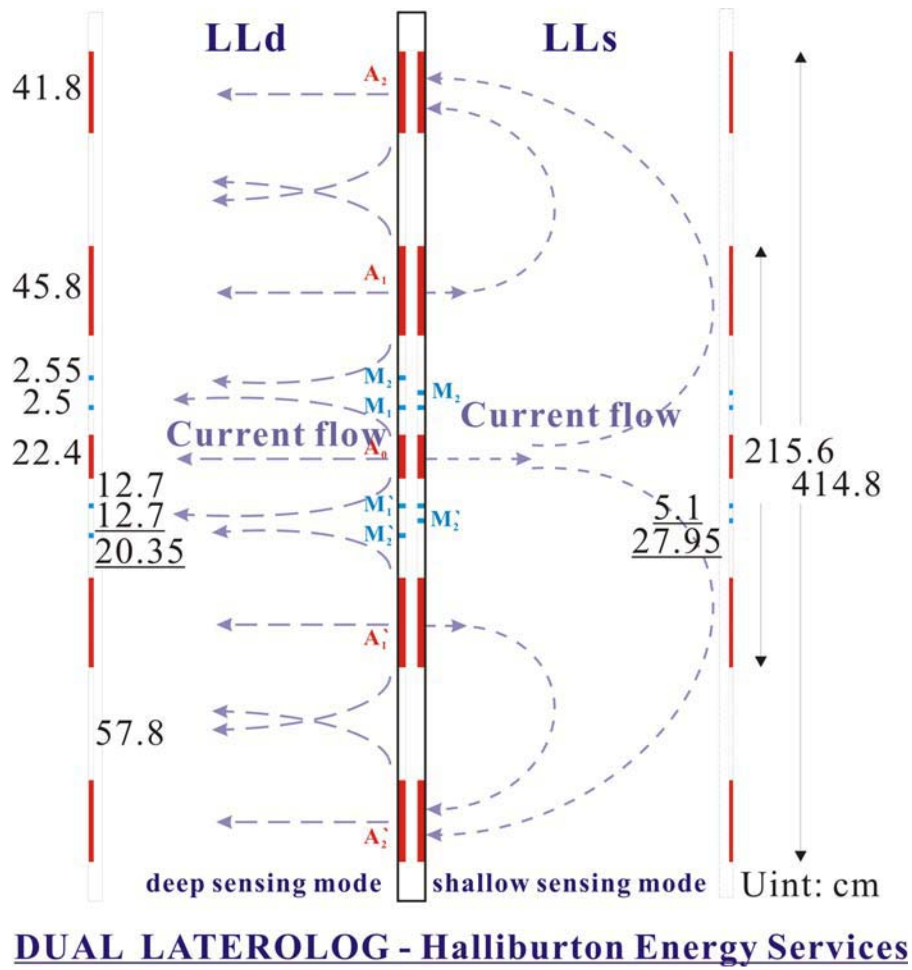

- **Determination of Intensities (W_j) of Bucking Currents**

Focusing Conditions

$$V(M_1) = V(M_2)$$
$$V(M_{1'}) = V(M_{2'})$$

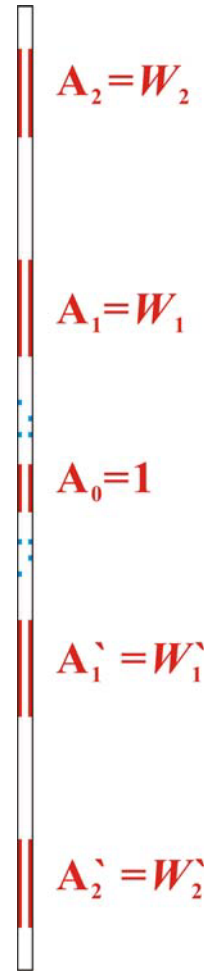

Post-Processing Method

Synthetic Focusing (Cozzolino et al, 2007)

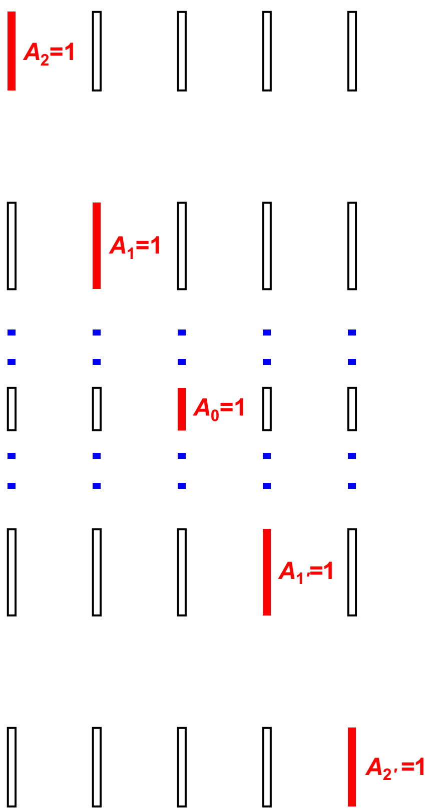

Total potential on M_i

→ Superposition principle

$$V(M_2) = W_2 V_{2,2} + W_1 V_{2,1} + V_{2,0} + W_{1'} V_{2,1'} + W_{2'} V_{2,2'}$$
$$V(M_1) = W_2 V_{1,2} + W_1 V_{1,1} + V_{1,0} + W_{1'} V_{1,1'} + W_{2'} V_{1,2'}$$
$$V(M_{1'}) = W_2 V_{1',2} + W_1 V_{1',1} + V_{1',0} + W_{1'} V_{1',1'} + W_{2'} V_{1',2'}$$
$$V(M_{2'}) = W_2 V_{2',2} + W_1 V_{2',1} + V_{2',0} + W_{1'} V_{2',1'} + W_{2'} V_{2',2'}$$

(1) Focusing conditions

$$V(M_1) = V(M_2)$$
$$V(M_{1'}) = V(M_{2'})$$

(2) Relationships between W_j

$$W_2 = (W_1 + c), \quad W_{2'} = (W_{1'} + c) \quad for \ \text{LLd}$$
$$W_2 = -(W_1 + c), \quad W_{2'} = -(W_{1'} + c) \quad for \ \text{LLs}$$

with $c = 0.5$

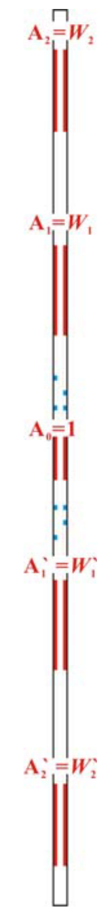

One problem with several RHSs

Embedded Post-Processing Method (EPPM)

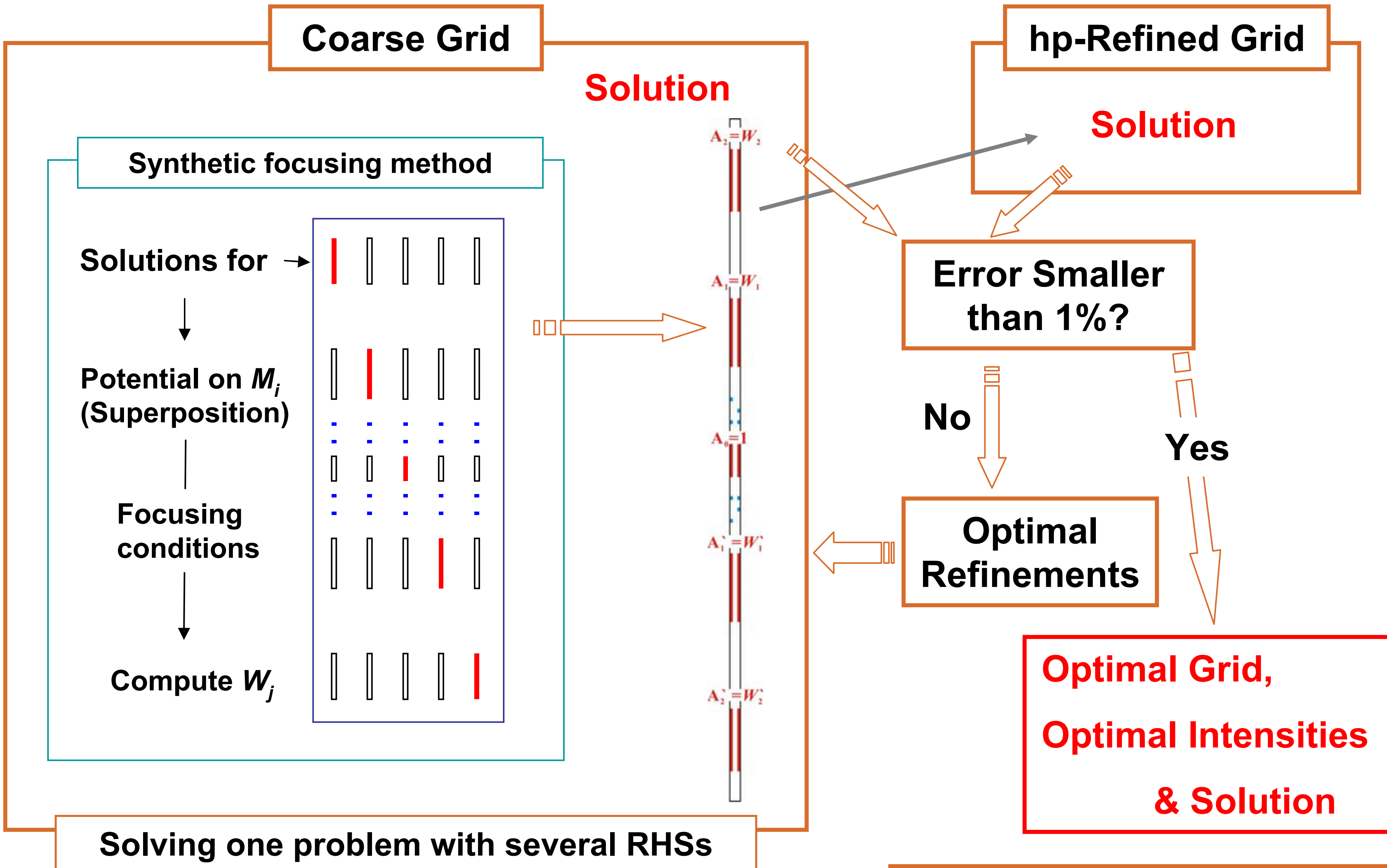

Simulating the DLL tool

Model

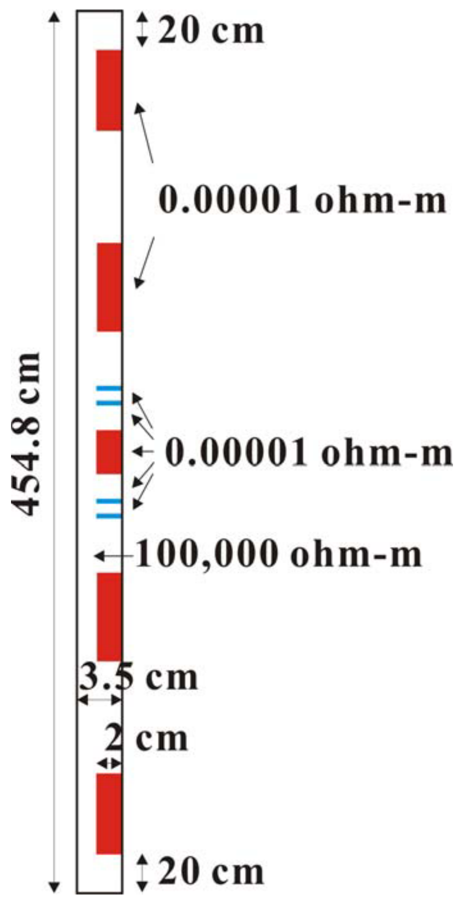

Using the Tool Configuration of Halliburton Energy Services' DLL

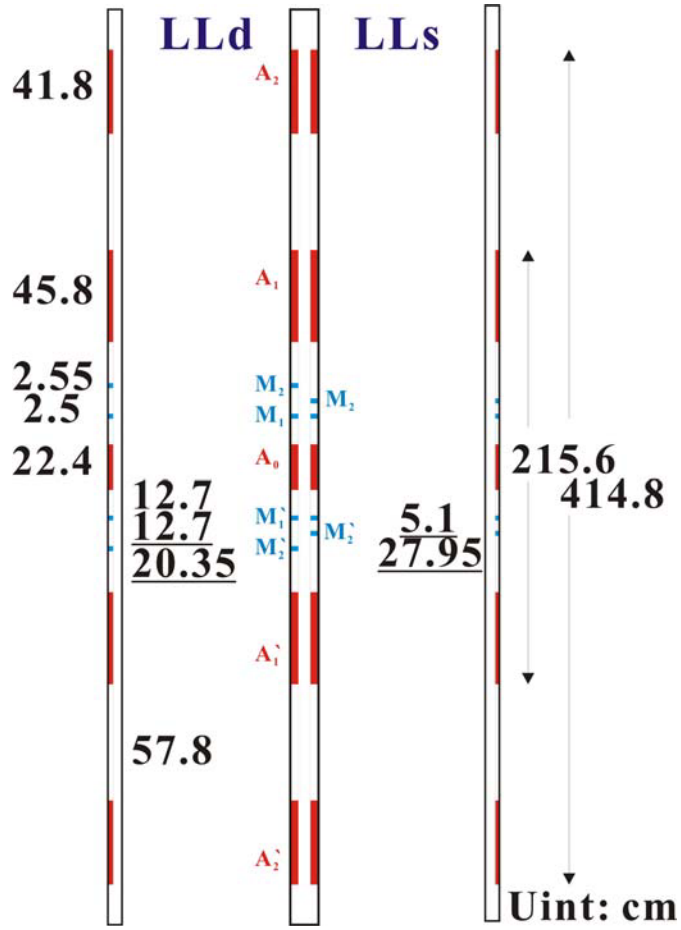

Invaded Formation (Vertical Well)

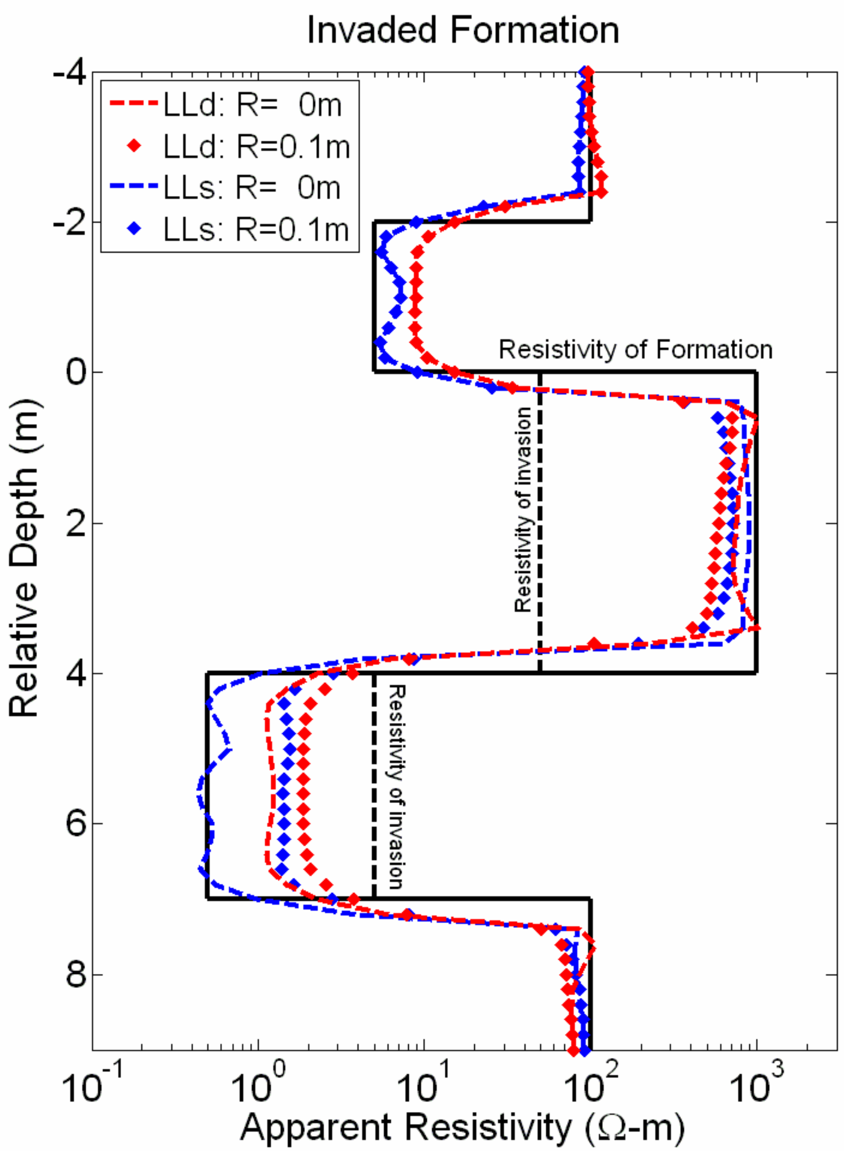

Effects of Invasion: LLs ↑

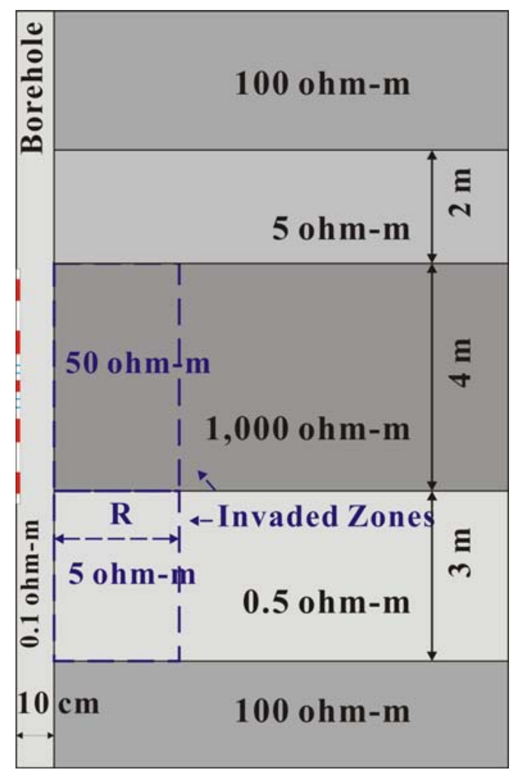

Borehole: 0.1 m in radius
0.1 ohm-m in resistivity

Anisotropic Formation (Vertical Well)

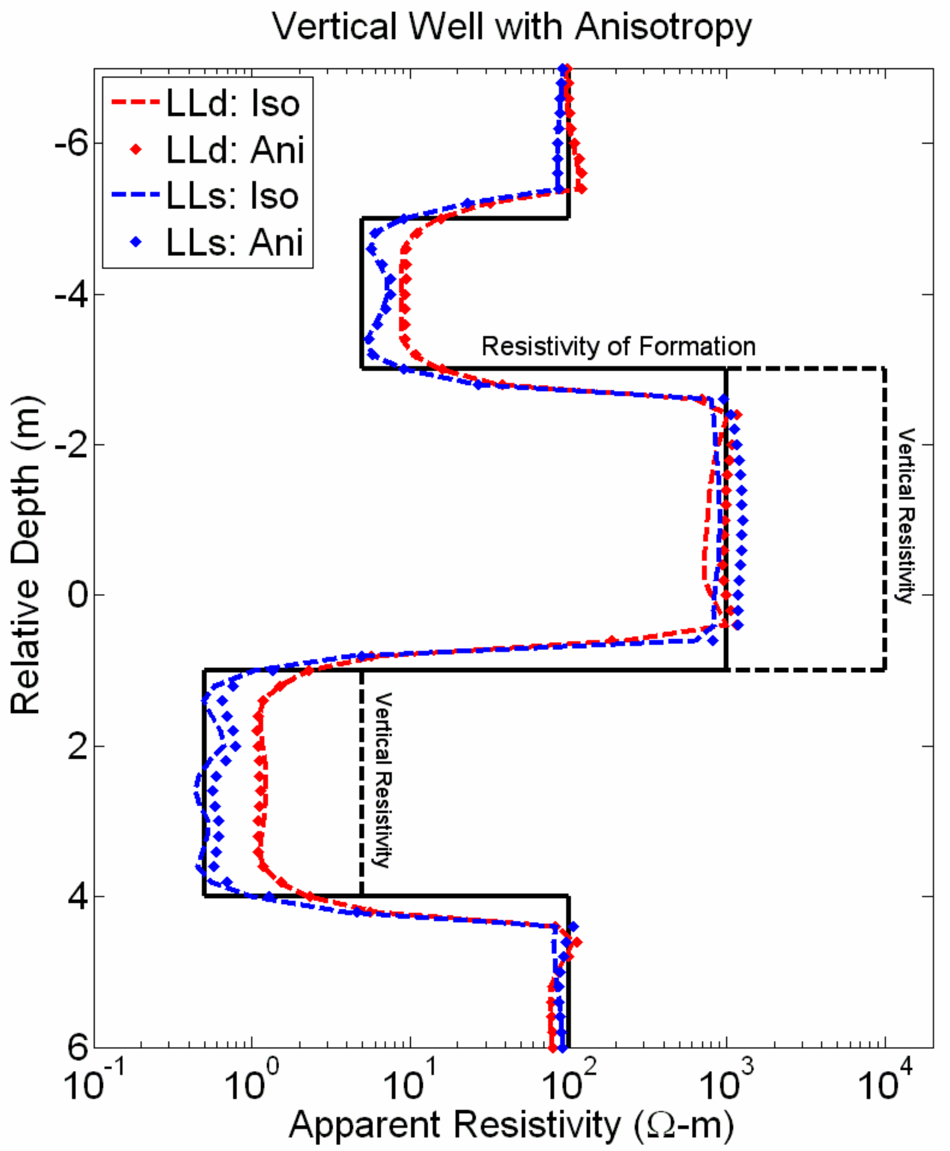

Effects of anisotropy: LLs ↑

LLd: effects of anisotropy are negligible in conductive layer

3D Methodology and DLL Simulations I

- **Deviated Wells**
  - Non-orthogonal system of coordinates
  - Fourier series expansion
  - Numerical results
- Eccentered Measurements
- Iterative Solver
- Parallel Implementation

3D Deviated Well

Cartesian system of coordinates: (x_1, x_2, x_3)

New non-orthogonal system of coordinates: $(\zeta_1, \zeta_2, \zeta_3)$

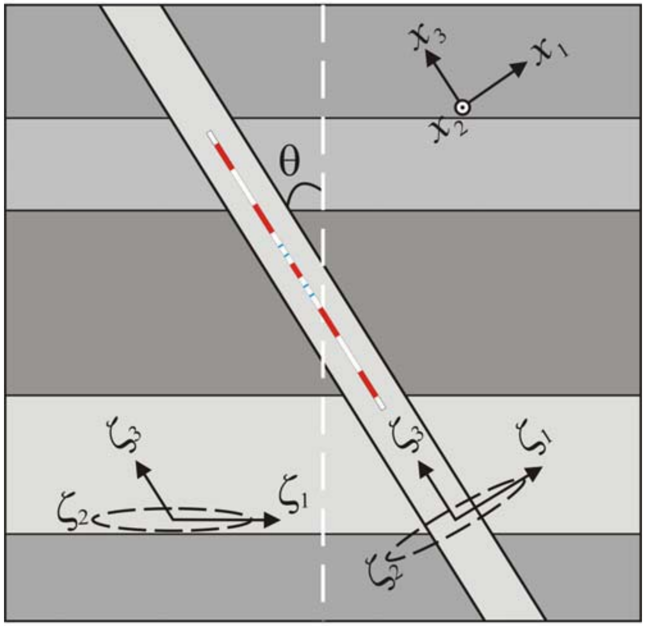

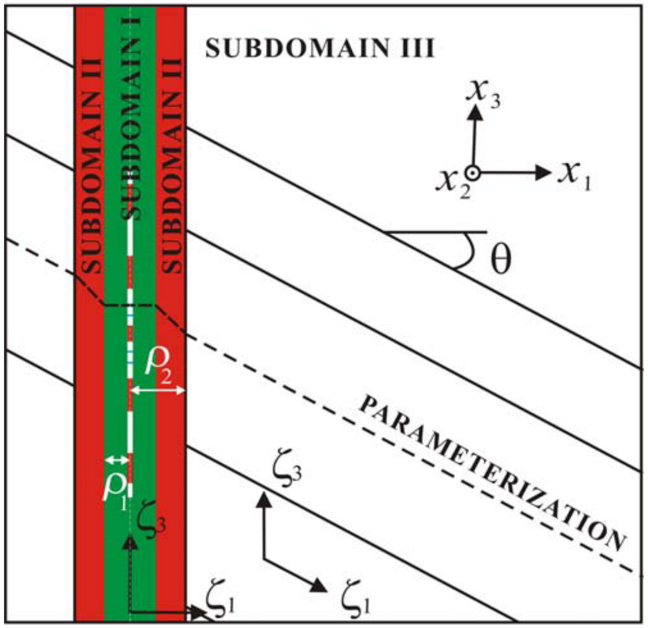

Subdomain I

$$\begin{cases} x_1 = \zeta_1 \cos\zeta_2 \\ x_2 = \zeta_1 \sin\zeta_2 \\ x_3 = \zeta_3 \end{cases}$$

Subdomain II

$$\begin{cases} x_1 = \zeta_1 \cos\zeta_2 \\ x_2 = \zeta_1 \sin\zeta_2 \\ x_3 = \zeta_3 + \tan\theta \dfrac{\zeta_1 - \rho_1}{\rho_2 - \rho_1} \rho_2 \cos\zeta_2 \end{cases}$$

Subdomain III

$$\begin{cases} x_1 = \zeta_1 \cos\zeta_2 \\ x_2 = \zeta_1 \sin\zeta_2 \\ x_3 = \zeta_3 + \zeta_1 \tan\theta \cos\zeta_2 \end{cases}$$

3D Deviated Well

Cartesian system of coordinates: (x_1, x_2, x_3)

New non-orthogonal system of coordinates: $(\zeta_1, \zeta_2, \zeta_3)$

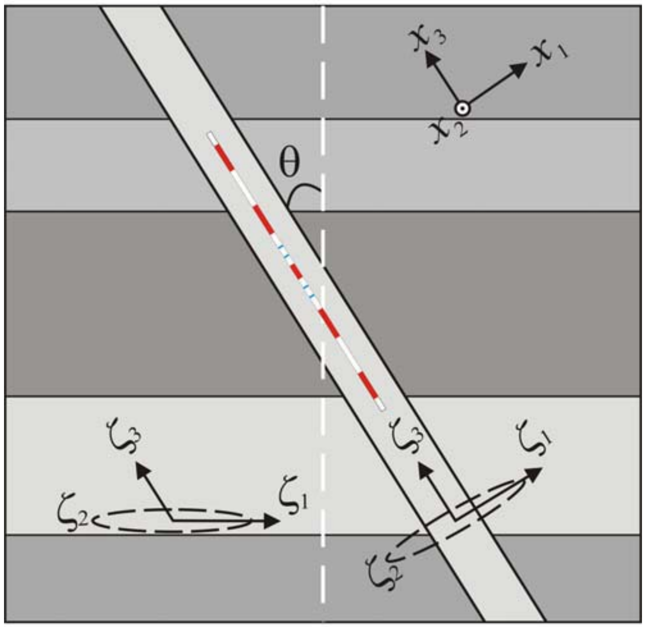

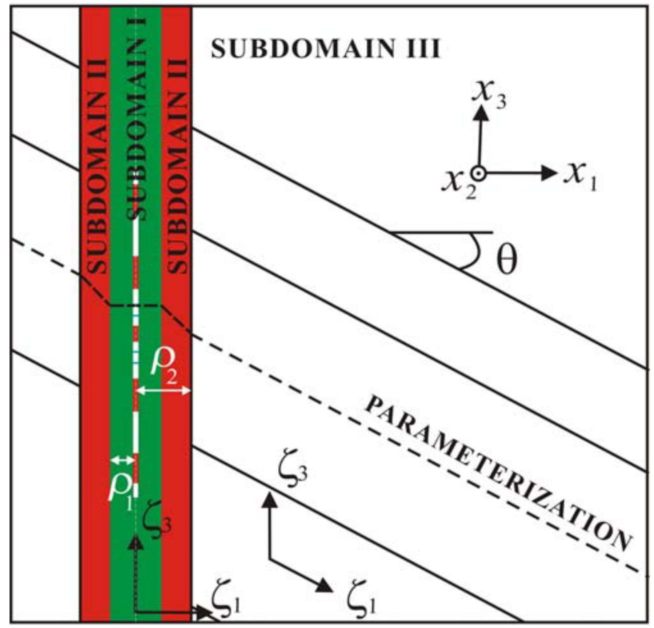

Constant material coefficients in the quasi-azimuthal direction ζ_2

in the new non-orthogonal system of coordinates!!!!

Final Variational Formulation

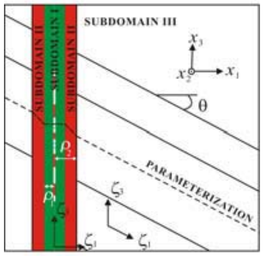

DC problem: $-\nabla \sigma \nabla u = f$

Define Jacobian : $\mathbf{J} = \left\{ \frac{\partial x_i}{\zeta_j} \right\}_{i,j=1,2,3}$

3D variational formulation in the new system of coordinates:

$$\begin{cases} \text{Find } \tilde{u} \in \underline{\tilde{u}}_D + \tilde{H}^1_D(\Omega) \text{ such that:} \\ < \frac{\partial \tilde{v}}{\partial \zeta}, \tilde{\boldsymbol{\sigma}}_{NEW} \frac{\partial \tilde{u}}{\partial \zeta} >_{L^2(\Omega)} = < \tilde{v}, \tilde{f}_{NEW} >_{L^2(\Omega)} + < \tilde{v}, \tilde{g}_{NEW} >_{L^2(\Omega)} \quad \forall \tilde{v} \in \tilde{H}^1_D(\Omega), \end{cases}$$

where

$$\tilde{\boldsymbol{\sigma}}_{NEW} := \mathbf{J}^{-1} \tilde{\boldsymbol{\sigma}} \mathbf{J}^{-1T} |\mathbf{J}| \qquad \tilde{f}_{NEW} := \tilde{f} \, |\mathbf{J}| \qquad \tilde{g}_{NEW} := \tilde{g} \, |\mathbf{J}_S|$$

The same concept can be applied to AC problems

Fourier Series Expansion in ζ_2

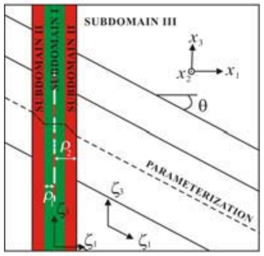

Fourier Series Expansion of a Function ω in ζ_2:

$$\omega = \sum_{l=-\infty}^{l=\infty} \omega_l e^{jl\zeta_2} = \sum_{l=-\infty}^{l=\infty} F_l(\omega) e^{jl\zeta_2}$$

Final Variational Formulation after Fourier Series Expansion in ζ_2:

$$\begin{cases} \text{Find } F_l(u) \in F_l(\underline{u}_D) + H_D^1(\Omega_{2D}) \text{ such that:} \\ \sum_{k=-\infty}^{k=\infty} \sum_{l=k-2}^{l=k+2} < F_k\left(\frac{\partial v}{\partial \zeta}\right), F_{k-l}(\sigma_{NEW}) F_l\left(\frac{\partial u}{\partial \zeta}\right) >_{L^2(\Omega_{2D})} \\ = \sum_{k=-\infty}^{k=\infty} \left[< F_k(v), F_k(f_{NEW}) >_{L^2(\Omega_{2D})} + < F_k(v), F_k(g_{NEW}) >_{L^2(\Omega_{2D})} \right] \quad \forall F_k(v) \in H_D^1(\Omega), \end{cases}$$

← **Mono-modal test function:**

$$v = v_k e^{jk\zeta_2}$$

because $F_{k-l}(\sigma_{NEW}) = 0$ **for every** $|k-l| > 2$.

Only Five Fourier Modes (l) are enough to represent σ_{NEW} EXACTLY for each k.

Therefore, we need to truncate only Fourier Modes (k) for 3D solution.

Example (9 Fourier Modes)

9 Fourier Modes for the Solution: $-4 < k < 4$

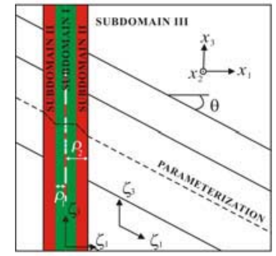

$$\sum_{k=-4}^{k=4}\sum_{l=k-2}^{l=k+2} < F_k\left(\frac{\partial v}{\partial \zeta}\right), F_{k-l}(\sigma_{NEW}) F_l\left(\frac{\partial u}{\partial \zeta}\right) >_{L^2(\Omega_{2D})}$$

$$= \sum_{k=-4}^{k=4}\left[< F_k(v), F_k(f_{NEW}) >_{L^2(\Omega_{2D})} + < F_k(v), F_k(g_{NEW}) >_{L^2(\Omega_{2D})} \right]$$

$$\Rightarrow \sum_{k=-4}^{k=4}\sum_{l=k-2}^{l=k+2} d_l^k F_l(u) = \sum_{k=-4}^{k=4} b_k(F_k(v))$$

d_l^k***: represents a 2D stiffness matrix***

$$\begin{bmatrix} d_{-4}^{-4} & d_{-3}^{-4} & d_{-2}^{-4} & 0 & 0 & 0 & 0 & 0 & 0 \\ d_{-4}^{-3} & d_{-3}^{-3} & d_{-2}^{-3} & d_{-1}^{-3} & 0 & 0 & 0 & 0 & 0 \\ d_{-4}^{-2} & d_{-3}^{-2} & d_{-2}^{-2} & d_{-1}^{-2} & d_{0}^{-2} & 0 & 0 & 0 & 0 \\ 0 & d_{-3}^{-1} & d_{-2}^{-1} & d_{-1}^{-1} & d_{0}^{-1} & d_{1}^{-1} & 0 & 0 & 0 \\ 0 & 0 & d_{-2}^{0} & d_{-1}^{0} & d_{0}^{0} & d_{1}^{0} & d_{2}^{0} & 0 & 0 \\ 0 & 0 & 0 & d_{-1}^{1} & d_{0}^{1} & d_{1}^{1} & d_{2}^{1} & d_{3}^{1} & 0 \\ 0 & 0 & 0 & 0 & d_{0}^{2} & d_{1}^{2} & d_{2}^{2} & d_{3}^{2} & d_{4}^{2} \\ 0 & 0 & 0 & 0 & 0 & d_{1}^{3} & d_{2}^{3} & d_{3}^{3} & d_{4}^{3} \\ 0 & 0 & 0 & 0 & 0 & 0 & d_{2}^{4} & d_{3}^{4} & d_{4}^{4} \end{bmatrix} \begin{bmatrix} F_{-4}(u) \\ F_{-3}(u) \\ F_{-2}(u) \\ F_{-1}(u) \\ F_{0}(u) \\ F_{1}(u) \\ F_{2}(u) \\ F_{3}(u) \\ F_{4}(u) \end{bmatrix} = \begin{bmatrix} b_{-4} \\ b_{-3} \\ b_{-2} \\ b_{-1} \\ b_{0} \\ b_{1} \\ b_{2} \\ b_{3} \\ b_{4} \end{bmatrix}$$

Verification of 3D Simulation

θ = 0, 30 and 60 degrees

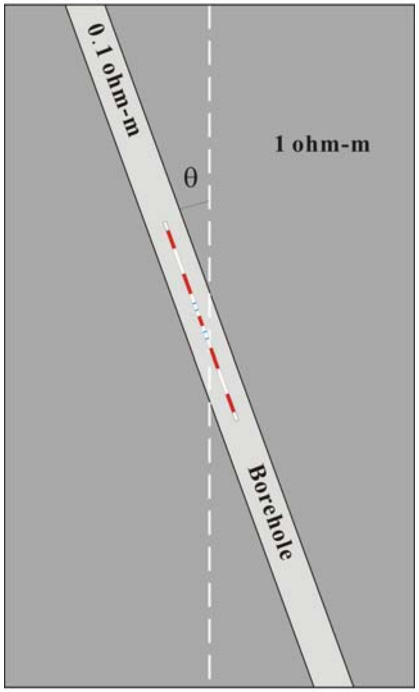

Relative errors of laterolog measurements in a homogeneous formation

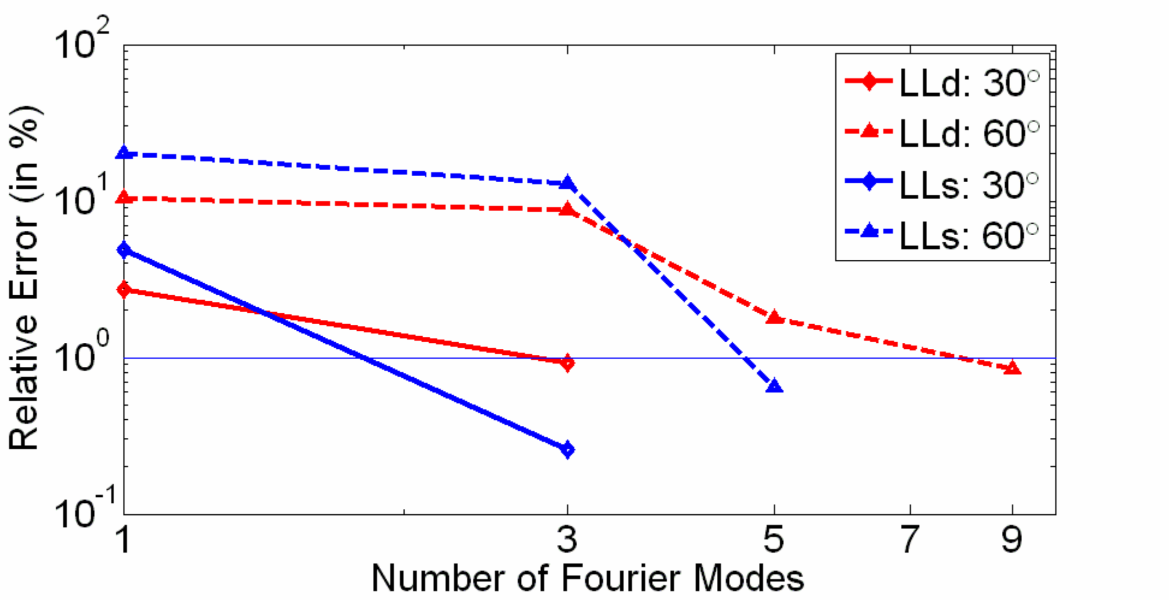

Reference Solutions: Solutions for 0° deviated well

Convergence History of LLd Logs

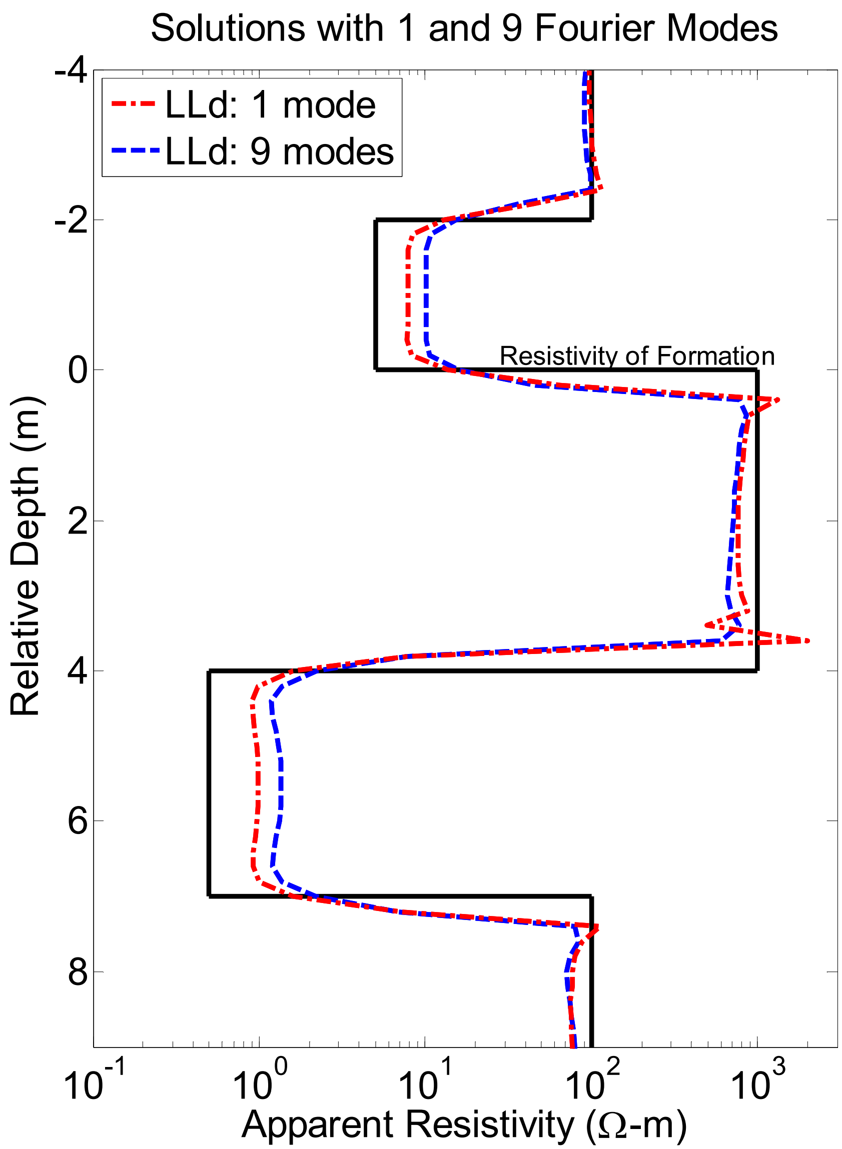

Dip angle: 45 degrees

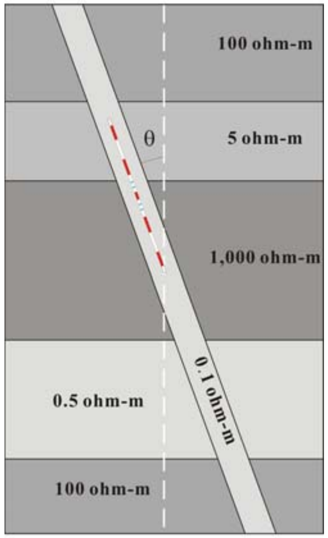

Convergence History of LLd Logs

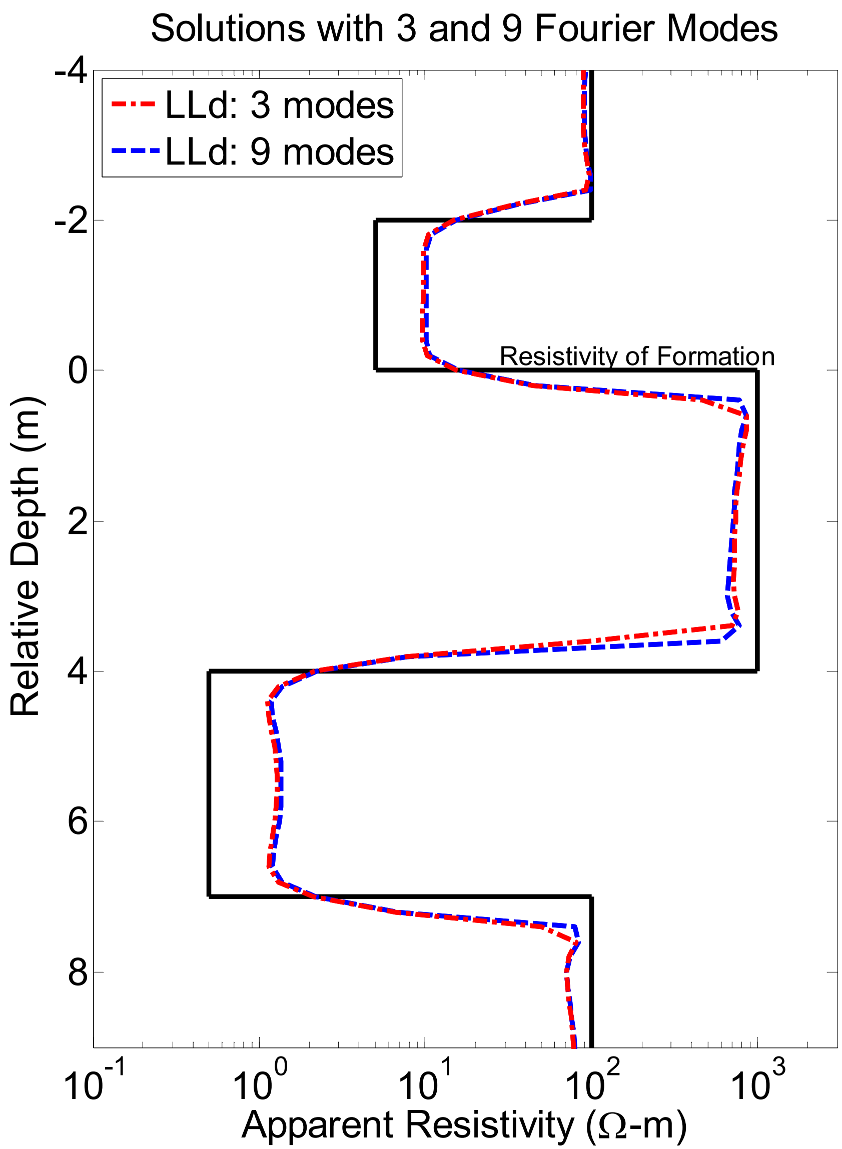

Dip angle: 45 degrees

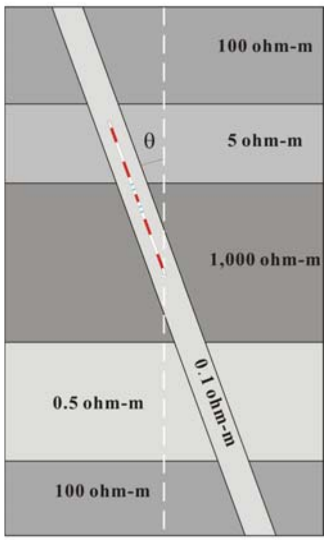

Convergence History of LLd Logs

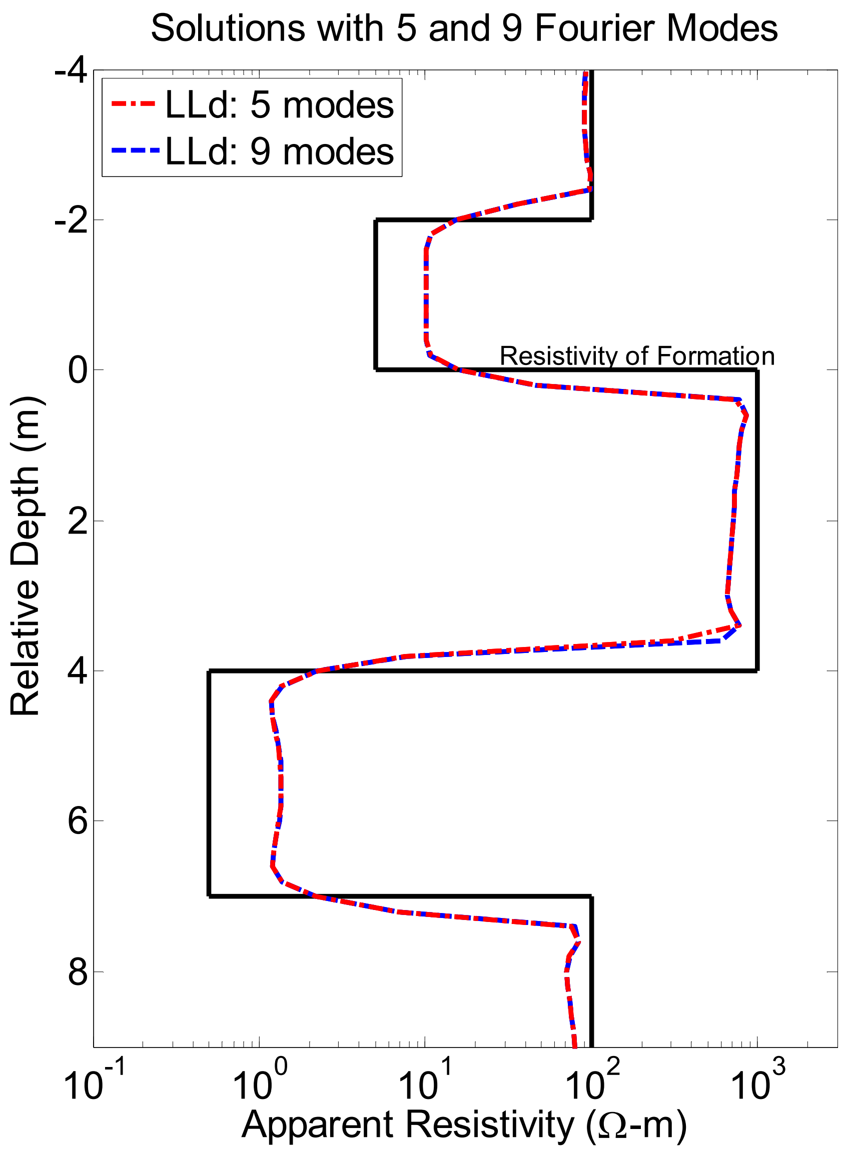

Dip angle: 45 degrees

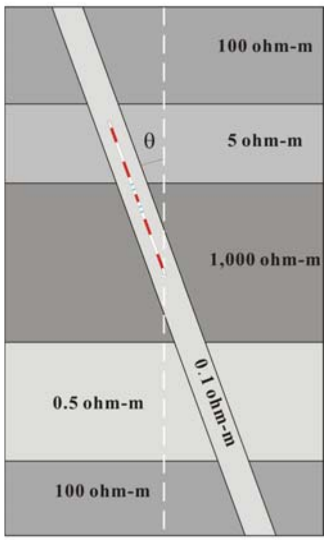

Convergence History of LLd Logs

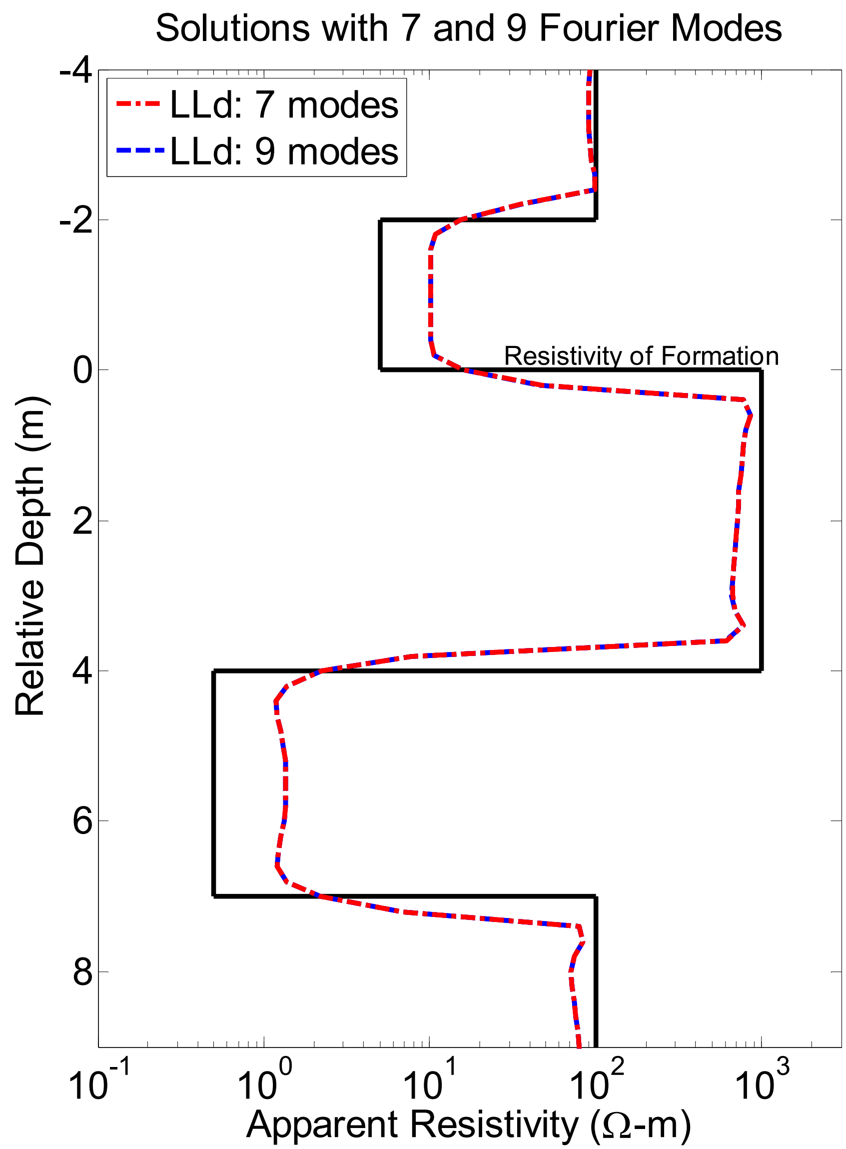

Dip angle: 45 degrees

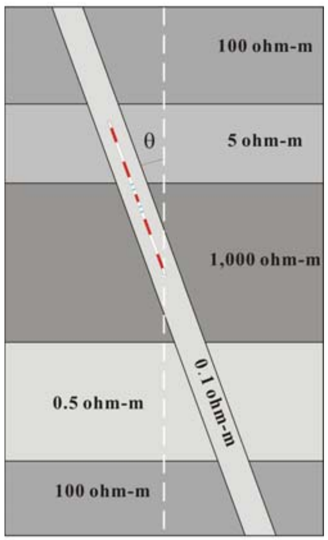

Deviated Well (60, 45 and 10 degrees)

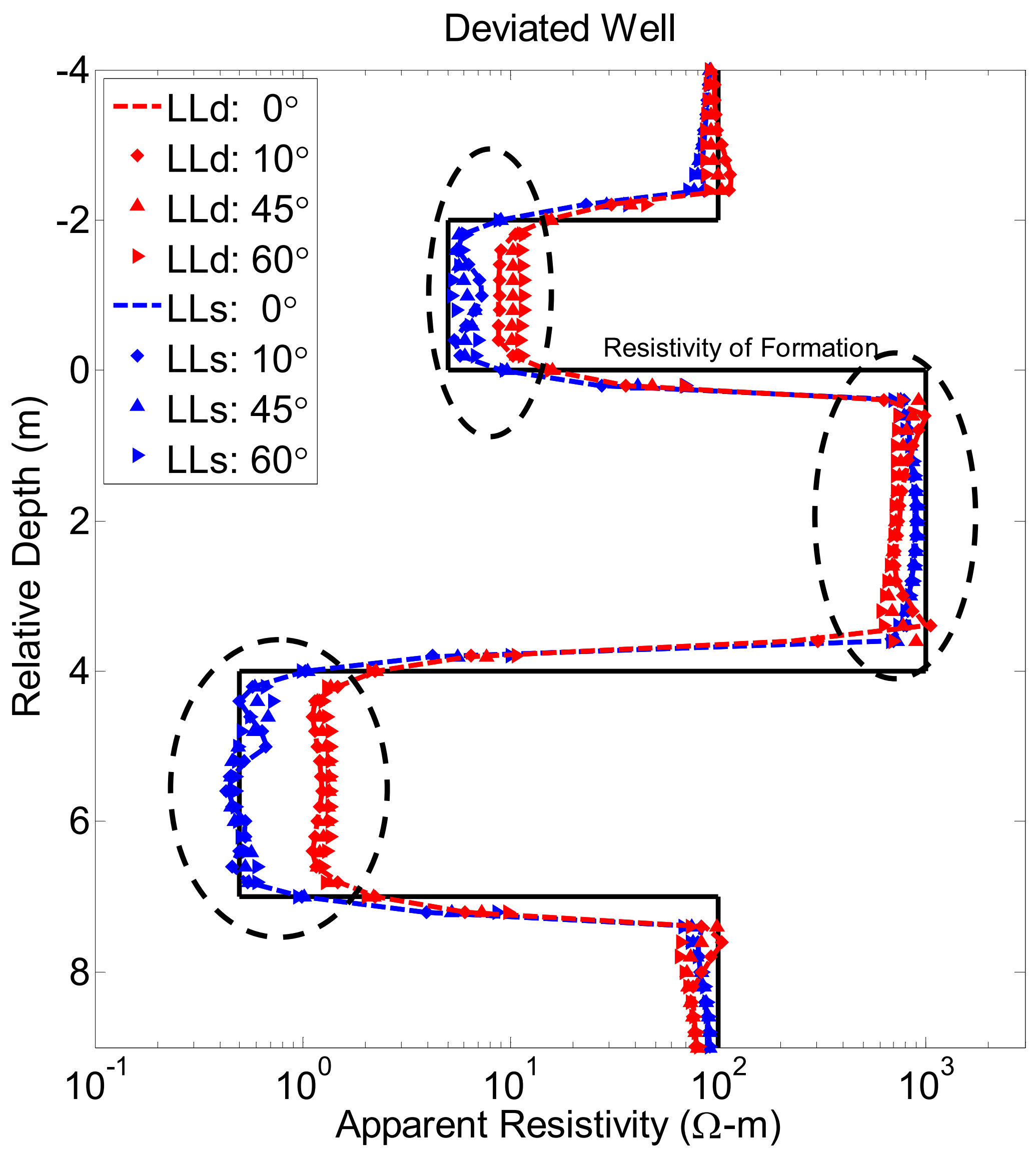

Effects of dip angle:

Thin layer ↑

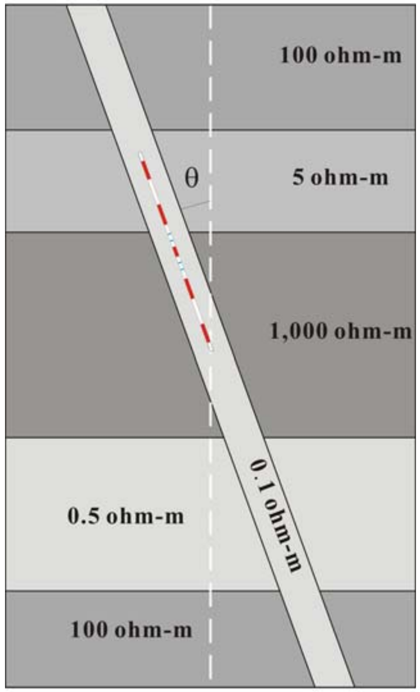

3D Methodology and DLL Simulations II

- Deviated wells
- <u>Eccented Measurements</u>
  - Non-orthogonal system of coordinates
  - Fourier series expansion
  - Numerical results
- Iterative Solver
- Parallel Implementation

3D Eccentered Well

New non-orthogonal system of coordinates: $(\zeta_1, \zeta_2, \zeta_3)$

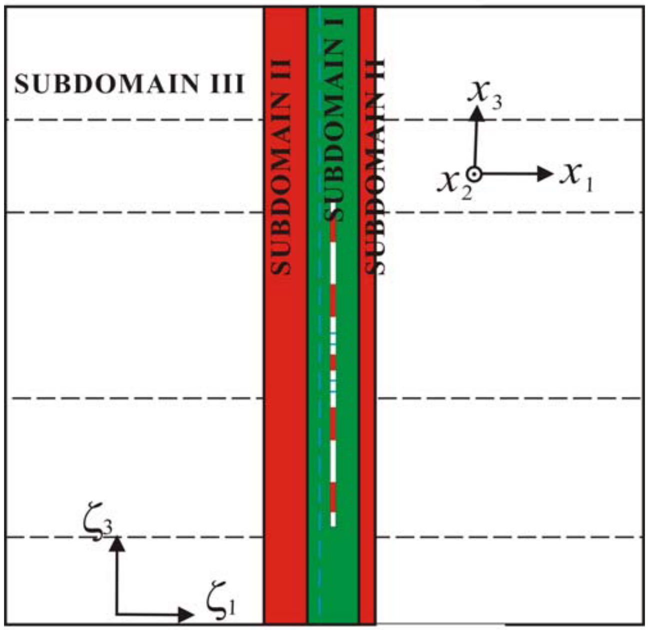

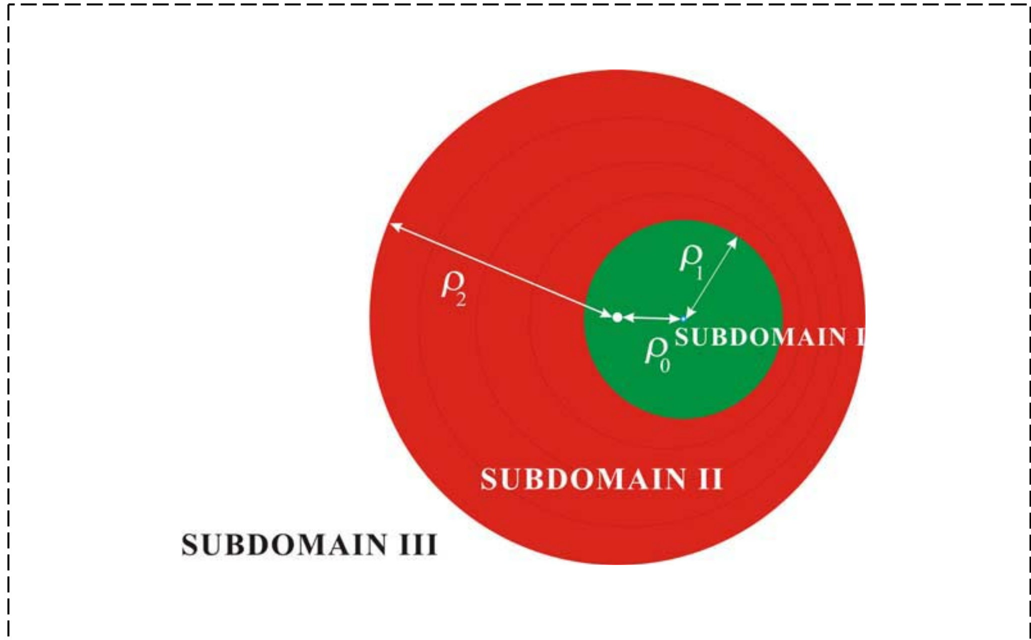

Subdomain I

$$\begin{cases} x_1 = \rho_0 + \zeta_1 \cos\zeta_2 \\ x_2 = \zeta_1 \sin\zeta_2 \\ x_3 = \zeta_3 \end{cases}$$

Subdomain II

$$\begin{cases} x_1 = \dfrac{\zeta_1 - \rho_2}{\rho_1 - \rho_2}\rho_0 + \zeta_1 \cos\zeta_2 \\ x_2 = \zeta_1 \sin\zeta_2 \\ x_3 = \zeta_3 \end{cases}$$

Subdomain III

$$\begin{cases} x_1 = \zeta_1 \cos\zeta_2 \\ x_2 = \zeta_1 \sin\zeta_2 \\ x_3 = \zeta_3 \end{cases}$$

Eccentricity

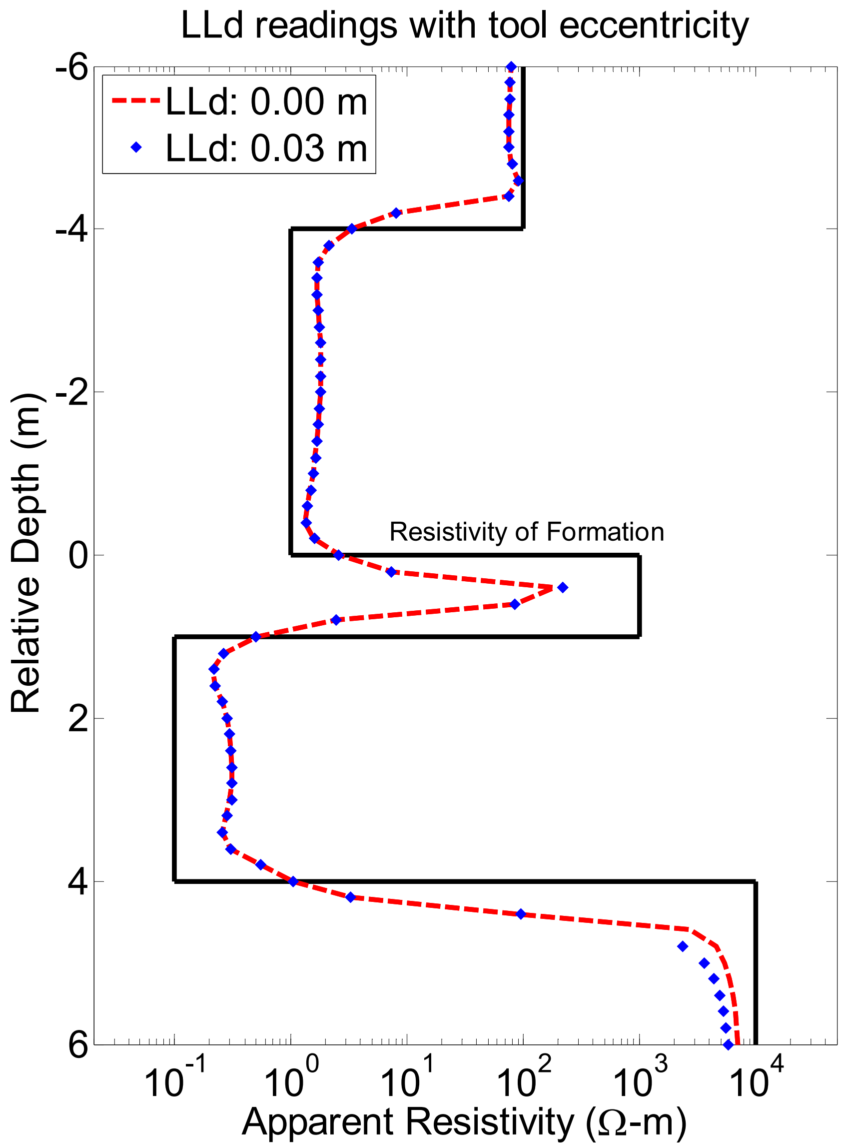

Effects of eccentricity: resistive layer ↑

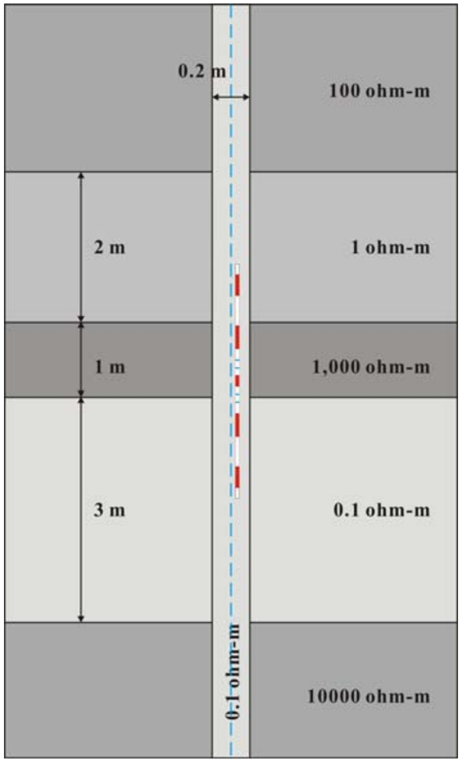

3D Methodology and DLL Simulations III

- Deviated Wells
- Eccentered Measurements
- **Iterative Solver**
  - 2D block Jacobi pre-conditioner
  - Numerical results
- Parallel Implementation

Iterative Solver I

Iterative Solver for Fast 3D Simulation:

- 2D Block Jacobi Pre-Conditioner

- Krylov-subspace optimization method (BI-Conjugate Gradient)

system of equations with 9 Fourier modes: (deviated well)

$$\begin{bmatrix} d_{-4}^{-4} & d_{-3}^{-4} & d_{-2}^{-4} & 0 & 0 & 0 & 0 & 0 & 0 \\ d_{-4}^{-3} & d_{-3}^{-3} & d_{-2}^{-3} & d_{-1}^{-3} & 0 & 0 & 0 & 0 & 0 \\ d_{-4}^{-2} & d_{-3}^{-2} & d_{-2}^{-2} & d_{-1}^{-2} & d_{0}^{-2} & 0 & 0 & 0 & 0 \\ 0 & d_{-3}^{-1} & d_{-2}^{-1} & d_{-1}^{-1} & d_{0}^{-1} & d_{1}^{-1} & 0 & 0 & 0 \\ 0 & 0 & d_{-2}^{0} & d_{-1}^{0} & d_{0}^{0} & d_{1}^{0} & d_{2}^{0} & 0 & 0 \\ 0 & 0 & 0 & d_{-1}^{1} & d_{0}^{1} & d_{1}^{1} & d_{2}^{1} & d_{3}^{1} & 0 \\ 0 & 0 & 0 & 0 & d_{0}^{2} & d_{1}^{2} & d_{2}^{2} & d_{3}^{2} & d_{4}^{2} \\ 0 & 0 & 0 & 0 & 0 & d_{1}^{3} & d_{2}^{3} & d_{3}^{3} & d_{4}^{3} \\ 0 & 0 & 0 & 0 & 0 & 0 & d_{2}^{4} & d_{3}^{4} & d_{4}^{4} \end{bmatrix} \begin{bmatrix} F_{-4}(u) \\ F_{-3}(u) \\ F_{-2}(u) \\ F_{-1}(u) \\ F_{0}(u) \\ F_{1}(u) \\ F_{2}(u) \\ F_{3}(u) \\ F_{4}(u) \end{bmatrix} = \begin{bmatrix} l_{-4} \\ l_{-3} \\ l_{-2} \\ l_{-1} \\ l_{0} \\ l_{1} \\ l_{2} \\ l_{3} \\ l_{4} \end{bmatrix}$$

2D Block Jacobi Pre-Conditioner:

$$\begin{bmatrix} d_{-4}^{-4} & 0 & 0 & 0 & 0 & 0 & 0 & 0 & 0 \\ 0 & d_{-3}^{-3} & 0 & 0 & 0 & 0 & 0 & 0 & 0 \\ 0 & 0 & d_{-2}^{-2} & 0 & 0 & 0 & 0 & 0 & 0 \\ 0 & 0 & 0 & d_{-1}^{-1} & 0 & 0 & 0 & 0 & 0 \\ 0 & 0 & 0 & 0 & d_{0}^{0} & 0 & 0 & 0 & 0 \\ 0 & 0 & 0 & 0 & 0 & d_{1}^{1} & 0 & 0 & 0 \\ 0 & 0 & 0 & 0 & 0 & 0 & d_{2}^{2} & 0 & 0 \\ 0 & 0 & 0 & 0 & 0 & 0 & 0 & d_{3}^{3} & 0 \\ 0 & 0 & 0 & 0 & 0 & 0 & 0 & 0 & d_{4}^{4} \end{bmatrix}$$

d_l^k: *represents a 2D stiffness matrix*

Iterative Solver II (results)

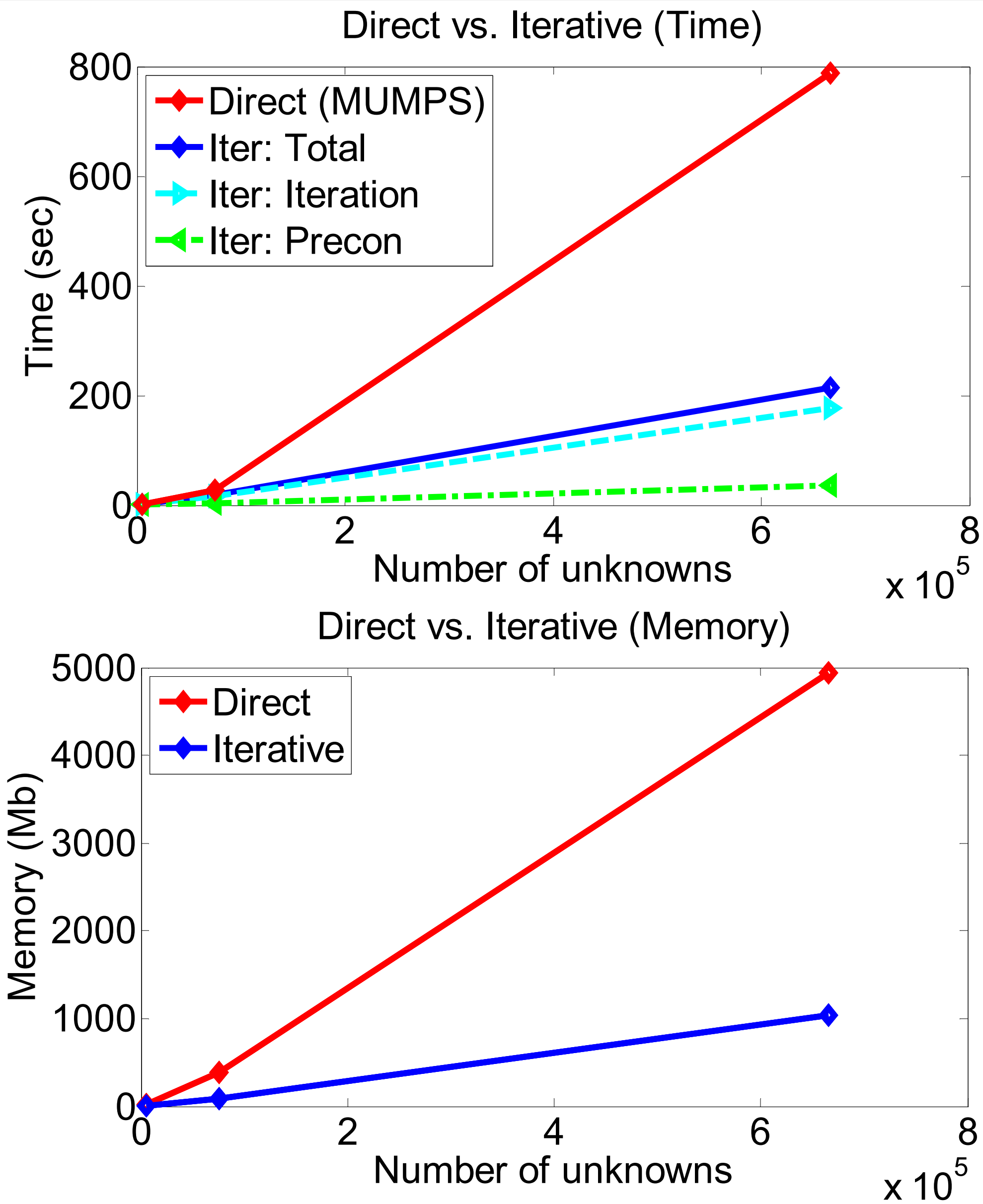

θ= 60 degrees

7 Fourier modes for solution

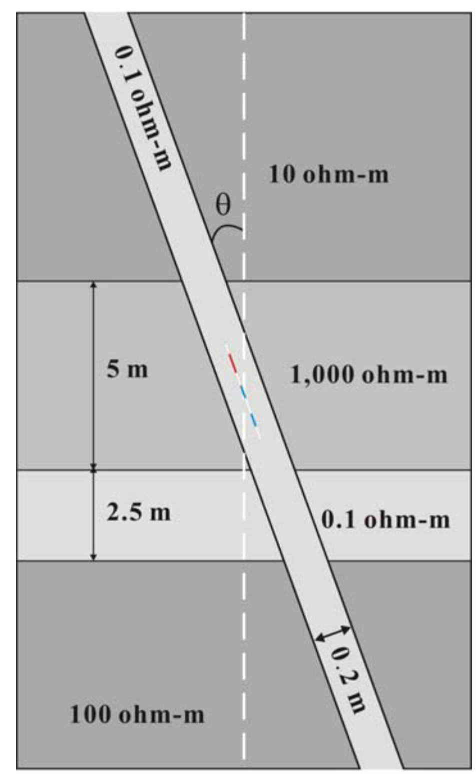

3D Methodology and DLL Simulations IV

- Deviated wells
- Eccentered Measurements
- Iterative Solver
- **Parallel Implementation**
  - Shared domain decomposition
  - Numerical results

3D Parallelization Implementation

Distributed Domain Decomposition

Shared Domain Decomposition!!

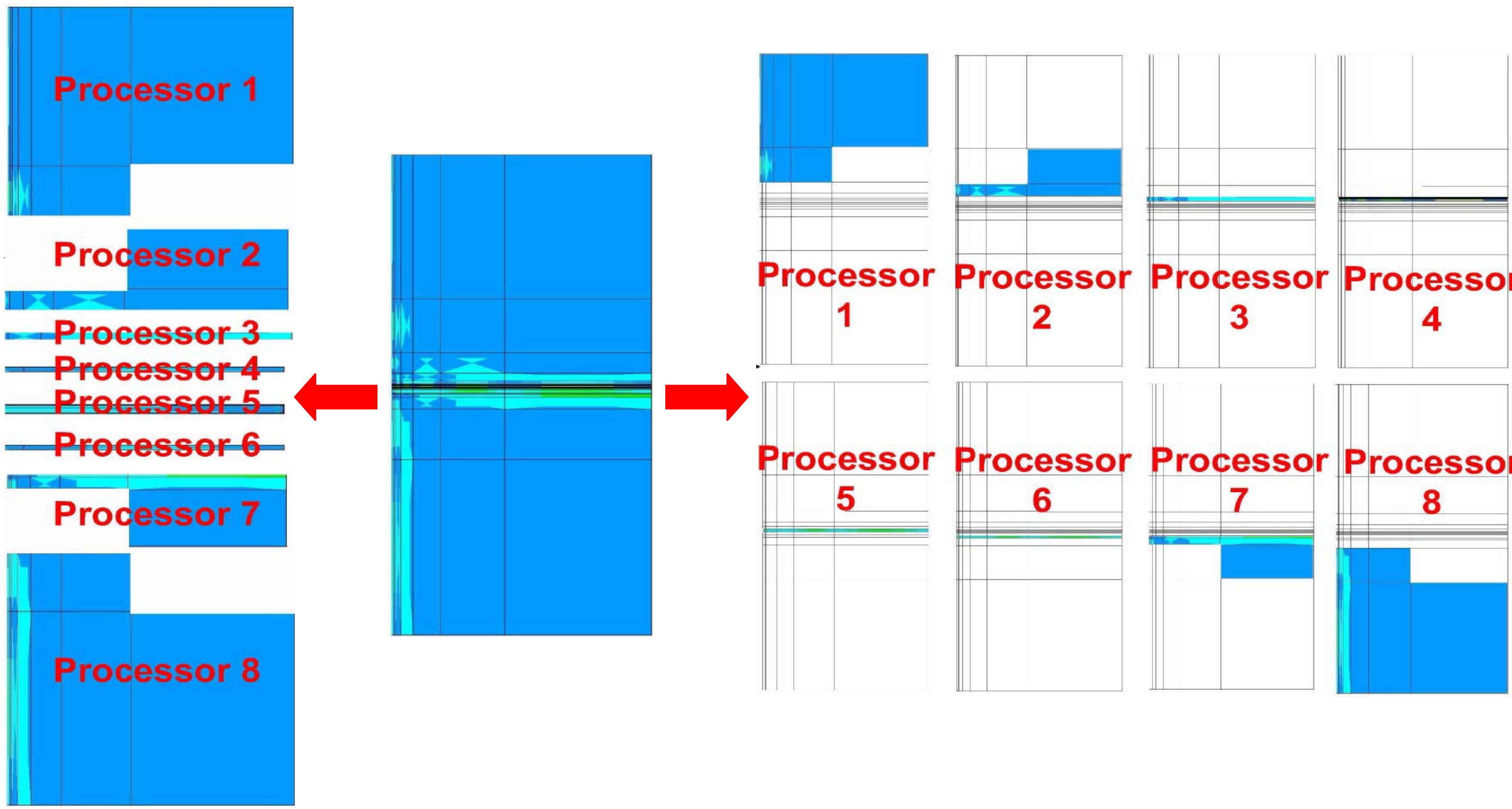

3D Parallelization Implementation

Scalability of the Parallel Multi-Frontal Solver (Direct Solver)

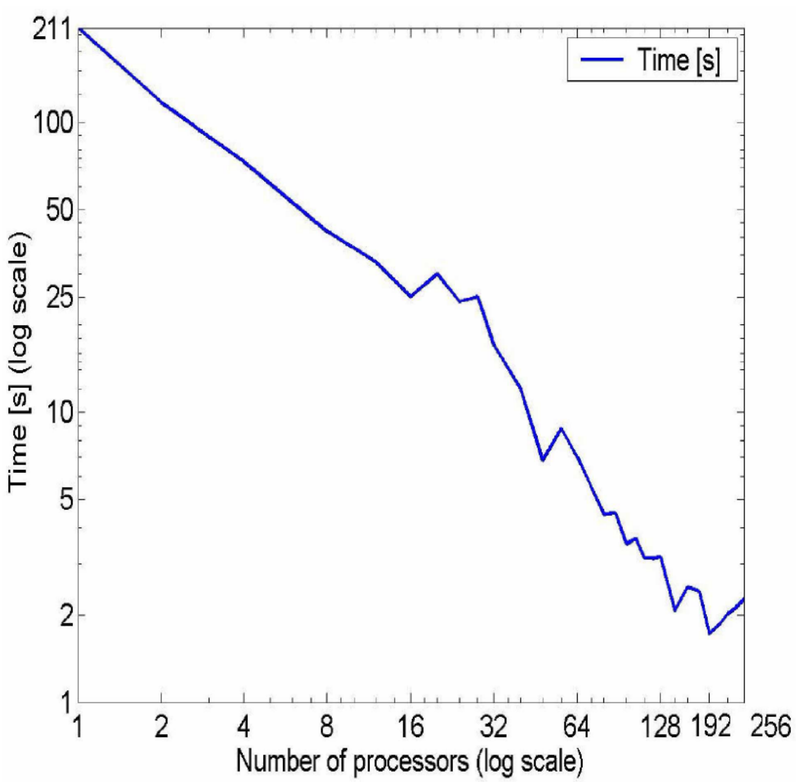

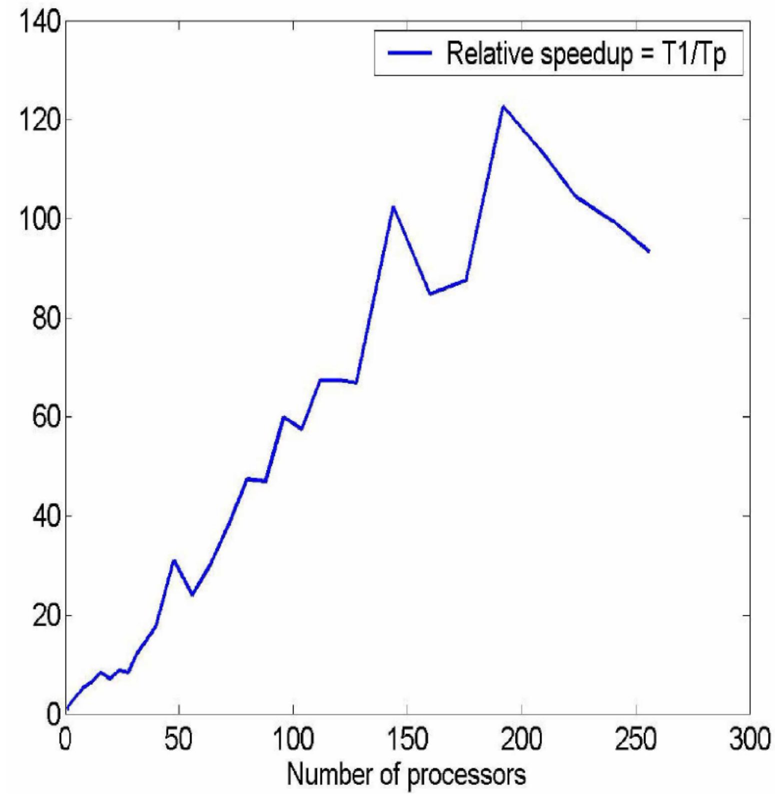

Parallel computations performed on Texas Advance Computing Center (TACC) 60% relative efficiency up to 200 processors.

Parallel direct solver is 125 times faster on 200 processors.

Conclusions

- We have successfully simulated 3D DLL measurements by combining the use of a Fourier series expansion in a non-orthogonal system of coordinates with a 2D higher-order self-adaptive *hp* finite element method, and by using an embedded post-processing method.

- Iterative Solver for Fast 3D Simulation.

- Parallelization of Direct Solver

Future Work

- Simulation of Non-Zero Dual-Laterolog Measurements
- Simulation of Highly Eccentered Measurements
- Parallelization of Iterative Solver.
- Multi-Frequency and Time-Domain Simulations
- User Friendly Interface
  - For setting up DLL tools and formations
  - For implementing new monitoring conditions

Acknowledgments

Sponsors of UT Austin's consortium on Formation Evaluation:

Anadarko Petroleum Corporation
ارامكو السعودية Saudi Aramco
Baker Hughes Baker Atlas
bhpbilliton
bp
Chevron
ConocoPhillips
Agip
Eni
ExxonMobil
HALLIBURTON
IMP Innovar INSTITUTO MEXICANO DEL PETRÓLEO
Marathon Oil Corporation
HYDRO
OXY occidental petroleum corporation
BR PETROBRAS
Schlumberger
Shell
STATOIL
TOTAL
Weatherford